Analyses of TCR clustering at the T cell–antigen-presenting cell interface and its impact on the activation of naive CD4+ T cells

Silvia Pastor[1], Carlos G. Vaccaro[1], Alfredo Minguela[1,2], Raimund J. Ober[1,3] and **E. Sally Ward[1,4]**

[1]Center for Immunology, University of Texas Southwestern Medical Center, 6000 Harry Hines Boulevard, Dallas, TX 75390-9093, USA
[2]Immunology Service, University Hospital 'Virgen de la Arrixaca', El Palmer, Murcia, Spain
[3]Department of Electrical Engineering, University of Texas at Dallas, Richardson, TX 75080, USA
[4]Cancer Immunobiology Center, University of Texas Southwestern Medical Center, 6000 Harry Hines Boulevard, Dallas, TX 75390-8576, USA

Abstract

The role of micrometer-scale clustering of TCRs at the T cell–antigen-presenting cell (APC) interface in T cell activation is an area of active investigation. Here we have investigated the impact of variations in the extent of TCR clustering on the activation of naive CD4+ T cells. These T cells are derived from transgenic (tg) mice expressing TCRs (172.10 and 1934.4) specific for the N-terminal nonapeptide of MBP bound to I-A^u, and are associated with murine experimental autoimmune encephalomyelitis (EAE). The 172.10 TCR has a ~4-fold higher affinity for antigen relative to the 1934.4 TCR, allowing us to compare the properties of two tg T cells of different avidities. We observe that variations in large-scale TCR clustering at the T cell–APC interface do not correlate well with the extent of activation (CD25 or CD69 up-regulation and IL-2 or IFN-γ production). Efficient activation can also be achieved in the absence of micrometer-scale TCR clustering, indicating that this is not a prerequisite for the effective stimulation of naive T cells.

Introduction

Following TCR recognition of peptide–MHC (pMHC) antigen on the surface of antigen-presenting cells (APCs) or in artificial lipid bilayers, TCRs, protein kinase C (PKC)-θ and other signaling/co-stimulatory molecules can localize to the center of an organized structure called the immunological synapse (IS) (1–6). The IS comprises a central supramolecular activation cluster (cSMAC) of TCRs and PKCθ surrounded by a peripheral SMAC of leukocyte function-associated antigen (LFA)-1 and talin (1, 2). IS formation has been proposed to enhance TCR signaling by concentrating TCRs in a phosphatase-depleted region at the T cell–APC interface (1, 5, 7, 8). However, recent studies have shown that TCR microclusters form at the periphery of the IS and play a role in sustained signaling following a short period of signaling at the center of the IS (9, 10), leading to the suggestion that the central zone may serve to stabilize T cell–APC interactions (9). In addition, several analyses indicate that the IS serves a 'platform' function to integrate co-stimulatory or CD40–CD40L signals (11–14). Using a combination of *in silico* and experimental

studies, models in which the IS balances TCR signaling by enhancing TCR internalization/degradation have also been proposed (15).

The low numbers, ranging from 1 to 400 agonist pMHC complexes (16–22), that have been reported to be necessary to activate T cells suggest that the large-scale TCR clustering frequently observed under the conditions used to analyze cSMAC formation may be well above the threshold needed for the triggering of a T cell response. This is also consistent with studies showing that large-scale re-organization of TCRs and other components to form a mature IS at the T cell–APC interface is not necessary for the activation of CD4+ or CD8+ T cells (14, 22–25). Importantly, however, in analyses where only 10 pMHC complexes at the T cell–APC interface are sufficient to activate CD4+ T cells, aggregation of ICAM-1 into a ring typical of IS formation is observed (20). Similarly, microtubule repolarization occurs during induction of CD8+ T cell cytolytic activity in the absence of mature IS formation (22–24). Taken together with earlier observations that LFA-1

and talin re-organization can occur in the absence of large-scale TCR clustering (20, 26), the data suggest that cytoskeletal and adhesive effects necessary to stabilize T cell–APC conjugates occur at lower stimulatory thresholds than those required to induce large-scale TCR aggregation into the cSMAC.

In the current study, we have analyzed the effect of variations in the extent of TCR clustering at the T cell–APC interface on naive T cell activation, as this relates directly to the initiation of the immune response. We have used two populations of naive CD4$^+$ T cells associated with murine experimental autoimmune encephalomyelitis (EAE). These T cells are derived from mice transgenically expressing two TCRs (172.10 and 1934.4) (27, 28) specific for the N-terminal immunodominant epitope of MBP associated with the MHC class II molecule, I-A^u (29–31). In this model, autoreactive MBP1–9:I-A^u-specific T cells escape central tolerance induction due to the low affinity of the MBP epitope for restricting MHC, and higher affinity 'superagonist' analogs of the MBP epitope have been defined (32–35). In earlier studies, we have determined the affinities of the corresponding TCR–pMHC interactions using soluble recombinant molecules and surface plasmon resonance (36). The dissociation constant for the 172.10 TCR–pMHC interaction is 8.8 μM, whereas that of the lower affinity 1934.4 TCR–pMHC complex is 34.6 μM (36). This knowledge gives us the opportunity to assess the effects of TCR clustering using T cells where the affinities for cognate ligand are well defined.

As indicators of activation in the current study, we have analyzed CD25 and CD69 up-regulation, in addition to cytokine production. In contrast to very early events, these indicators are directly related to the effector function of T cells. We observe that in general, there is not a good correlation between the extent of TCR clustering and T cell activation. Where an impact of an increase in clustering is observed, it is manifested as slight down-regulatory effects at early stages of activation that in general do not translate into effects at later stages. In addition, we show that naive CD4$^+$ T cells can be efficiently activated in the absence of large-scale TCR clustering.

Methods

Transgenic mice

Mice transgenic (tg) for the 172.10 (27) and 1934.4 (28) TCRs, backcrossed onto the B10.PL (H-2^u) background for at least 10–15 generations, were generously provided by Joan Goverman and Hugh McDevitt, respectively. The 172.10 tg mice were maintained by intercrossing tg mice expressing the 172.10 TCRα and -β chains as described (27). The 1934.4 tg mice were maintained by backcrossing mice tg for the TCRαβ onto B10.PL mice. All mice were bred in the Animal Resource Center at the University of Texas Southwestern Medical Center under specific pathogen-free conditions. All studies were approved by the Institutional Animal Care and Research Advisory Committee.

Cell lines and reagents

The I-A^u-expressing B cell line, PL-8, (37) and 1934.4 T cell hybridoma (38) were kindly provided by David Wraith (University of Bristol, UK). Anti-mouse PerCP-labeled anti-CD4 (RM4-5), PE-labeled anti-CD4 (GK1.5), APC-labeled anti-CD4 (RM4-5), FITC-labeled anti-Vα2 (B20.1), PE-labeled anti-Vβ8 (F23.1), PE-labeled anti-CD45R/B220 (RA3-6B2), APC-labeled anti-CD3ε (145-2C11), FITC-labeled anti-CD69 (H1.2F3), APC-labeled anti-CD25 (PC61), APC-labeled anti-CD62L (Mel-14) and FITC-labeled anti-CD62L (Mel-14) antibodies were purchased from PharMingen or Caltag. Hybridomas expressing antibodies specific for CD16/CD32 (FcγRII and FcγRIII) (2.4G2), keyhole limpet hemocyanin (KLH) (hamster IgG2 control), mouse TCR Cβ (H57-597), [hamster IgG2 (39)] and I-A^u [10.2.16, (40)] were purchased from the American Type Cell Culture Collection. Antibodies were purified from culture supernatants using protein G-Sepharose. Purified anti-TCR Cβ (H57-597) was labeled with Alexa 488 (Molecular Probes) using methods recommended by the manufacturer.

The N-terminal nonapeptide of MBP (MBP1–9) and the position 4 analog MBP1–9[4Y] that binds to I-A^u with a higher affinity due to substitution of lysine at position 4 by tyrosine (32–34) were synthesized at the Protein Chemistry Technology Center, University of Texas Southwestern Medical Center (Dallas, TX, USA).

ELISA

Anti-IL-2 capture, biotinylated anti-IL-2 antibodies (JES6-1M2 and JES6-5H4, respectively) and anti-IFN-γ capture, biotinylated anti-IFN-γ antibodies (R4-6A2 and XMG1.2, respectively) for use in sandwich ELISAs were purchased from BD Biosciences, PharMingen Division (San Diego, CA, USA). Bound, biotinylated anti-IL-2 or anti-IFN-γ antibodies were detected using Extravidin–HRP conjugate (Sigma, St Louis, MO, USA). IL-2 concentrations were determined from standard curves generated using recombinant IL-2 (PharMingen, San Jose, CA, USA) in the ELISAs. ELISAs were carried out in triplicate and all data are shown as mean values. Statistical analyses were carried out using Student's t-test for a two-tailed distribution with unequal sample variance and values of $P < 0.05$ were considered to be significantly different.

Recombinant peptide–MHC complexes

Soluble, recombinant MBP peptide:I-A^u (MBP1–9[4Y]:1-A^u) complexes comprising the N-terminal peptide of MBP covalently tethered to I-A^u were generated and purified using baculovirus-infected High-Five cells (41). The position 4 analog with lysine substituted by tyrosine (32–34) was used, as complexes made with the lower affinity wild-type peptide are unstable (42). Recombinant protein was site specifically biotinylated and multimerized by addition of PE–Extravidin as described (42).

Analysis of binding of pMHC multimers to T cells

Single-cell suspensions of splenocytes isolated from naive tg mice were depleted of RBCs with lysis buffer (15 mM NH$_4$Cl, 0.1 mM KHCO$_3$, 0.1 mM Na$_2$EDTA pH 7.2–7.4) and washed twice with PBS. Cells were re-suspended in 1% BSA/PBS and incubated with 10 μg ml^{-1} anti-CD16/CD32 for 5 min on ice. Recombinant Extravidin–PE-labeled MBP1–9[4Y]:I-A^u complexes (6 μg ml^{-1}) and PerCP-labeled anti-CD4 antibody were

added, cells were incubated for 90 min at 12°C, washed twice with PBS and analyzed by flow cytometry. To assess TCR levels, tg T cells were stained with FITC-labeled anti-CD3ε antibody.

To assess the dissociation rates of MBP1–9[4Y]:I-A^u multimers from the 1934.4 TCR, 1934.4 T hybridoma cells (0.5×10^6 to 1×10^6 cells per sample) pre-treated with 2.5 µg ml^{-1} H57-597 or hamster isotype control (anti-KLH, IgG2) were incubated with MBP1–9[4Y]:I-A^u multimers for 90 min on ice, washed twice in PBS and an aliquot of cells removed to give the staining levels at the start of the dissociation experiment. The remainder of the cells were incubated with anti-I-A^u (10.2.16) antibody at a concentration of 100 µg ml^{-1} to block rebinding of dissociated MBP1–9[4Y]:I-A^u. Cells were incubated on ice for 10 or 20 min, washed and then analyzed for multimer staining levels. All flow cytometric analyses were carried out using a FACSCalibur^{BD} and WinMDI 2.8 (The Scripps Research Institute, La Jolla, CA, USA, http://facs.scripps.edu) for analysis. Dissociation of multimers was expressed as:

$$\frac{\text{MFI (background subtracted) at each time} \times 100\%}{\text{MFI (background subtracted) at time 0}}.$$

where MFI = mean fluorescence intensity.

Purification of CD4$^+$ T cells

We have observed that in some cases, T cells from 172.10 tg mice show an activated phenotype with >30% being CD62L^{lo} (assessed by flow cytometry using APC- or FITC-labeled anti-CD62L antibody). This was particularly the case for mice over 5 weeks of age. Only mice that had <10% CD62L^{lo} T cells were used as a source of naive T cells. CD4$^+$ T cells were purified by depletion using a Mouse CD4$^+$ T Cell Isolation Kit from Miltenyi Biotec (Auburn, CA, USA). Purity and CD62L status of the purified cells were verified by flow cytometry with PE-labeled anti-CD4 and APC- or FITC-labeled CD62L antibodies. In all studies described here, cells were 80–90% CD4$^+$ and ⩾90% CD62L^{hi}.

Analyses of TCR clustering

Purified cells were pre-treated with 10 µg ml^{-1} hamster isotype control (anti-KLH, IgG2) and 10 µg ml^{-1} anti-CD16/CD32 antibody to block FcγR binding for 10 min on ice, then split into two tubes and treated with either 2.5 µg ml^{-1} Alexa 488-labeled H57-597 or hamster isotype control. Irradiated or non-irradiated PL-8 cells (1×10^6 per well) treated with 10 µg ml^{-1} of anti-CD16/CD32 antibody and anti-KLH antibody (hamster IgG2) in phenol red-free cDMEM (10% FCS, 100 U ml^{-1} penicillin, 100 µg ml^{-1} streptomycin, 10 mM HEPES, 1 mM sodium pyruvate, 0.1 mM non-essential amino acids and 55 µM mercaptoethanol) were added to cover slides (Circular #1.5 12 mm, Fisherbrand) in 24-well plates and allowed to settle for 45 min. The medium was exchanged for medium containing different doses of MBP1–9 or MBP1–9[4Y] plus 2.5 µg ml^{-1} anti-CD16/CD32 antibody and 2.5 µg ml^{-1} anti-KLH antibody (hamster IgG2) to block FcγR binding. CD4$^+$ cells (1×10^6), treated as described above, were added to each well and cells were incubated for 1 h at 37°C. Following this, cells were washed with ice-cold PBS, fixed with 3.4% PFA for 30 min at room temperature, washed twice with PBS and incubated with PE-labeled anti-CD45R/B220 and APC-labeled anti-CD4 antibodies. Cells that were treated with isotype control were also incubated with Alexa 488-labeled H57-597. Cells were incubated with antibodies for 30 min at 4°C, washed twice in PBS and mounted in Prolong (Molecular Probes, Eugene, OR, USA).

Microscopy analyses

Cells were imaged using a Zeiss axiovert 200M epifluorescent inverted microscope using a cooled CCD camera (Orca ER, Hamamatsu, Bridgewater, NJ, USA) as described (43). Data were processed and displayed using a custom written software package in the high-level programing language Matlab (The Mathworks, Natick, MA, USA) (43). TCR clustering in acquired images was assessed visually and cells were categorized into one of three groups: unclustered, diffuse clustering or compact clustering. Representative examples of each of these groups are shown in Fig. 2.

Analyses of CD25 and CD69 up-regulation, cytokine production and TCR internalization

Naive, purified CD4$^+$CD62L^{hi} cells treated with either H57-597 (Alexa 488-labeled or unlabeled) or hamster isotype control (anti-KLH: IgG2) as for TCR clustering analyses were cultured in round-bottomed 96-well plates (10^5 cells per well) in the presence of irradiated PL-8 cells and different doses of MBP1–9, MBP1–9[4Y] or medium only (cDMEM containing 10% FCS). To block FcγR binding, 2.5 µg ml^{-1} anti-CD16/CD32 antibody and 2.5 µg ml^{-1} anti-KLH antibody (hamster IgG2) were added to PL-8 cells prior to addition of peptide.

For studies of CD25 and CD69 up-regulation, cells were harvested following 2, 4, 6 or 18 h incubation, washed twice with cold PBS and incubated with fluorescently labeled anti-CD69, anti-CD25 and anti-CD4 antibodies for 30 min on ice. Cells were washed twice with PBS and analyzed by flow cytometry. IL-2 or IFN-γ levels in culture supernatants following 24 or 72 h incubation, respectively, were quantitated by ELISA (above). To assess TCR internalization, cells were harvested following 4 h incubation with peptide-pulsed PL-8 cells. Cells were incubated with fluorescently labeled anti-CD4 and anti-CD3ε antibodies, washed as above and analyzed by flow cytometry. Surface TCR levels were expressed as:

$$\frac{\text{MFI for anti-CD3ε antibody staining levels for activated cells} \times 100\%}{\text{MFI for anti-CD3ε antibody staining levels for control cells}}.$$

All flow cytometry data were collected using a FACSCalibur^{BD} and data analyzed using WinMDI 2.8 (J. Trotter, Scripps Research Institute).

Results

Comparative analyses of TCR clustering by naive T cells that have different intrinsic affinities for peptide-MHC ligand

In earlier studies using surface plasmon resonance, we showed that the affinity of the 172.10 TCR is ~4-fold higher [K_D = 8.8 µM versus 34.6 µM (36)] than that of the 1934.4 TCR

for cognate pMHC (N-terminally acetylated MBP1–9 associated with I-A^u) (36). Consistent with this affinity difference, fluorescently labeled MBP1–9[4Y]:I-A^u multimers stain CD4$^+$ T cells that transgenically express the 172.10 TCR (172.10 tg T cells) to higher levels than those transgenically expressing the 1934.4 TCR (1934.4 tg T cells) (Fig. 1). We first assessed the effect of this affinity difference on large-scale clustering of TCRs at the T cell–APC interface when naive, tg T cells were added to peptide-pulsed APCs.
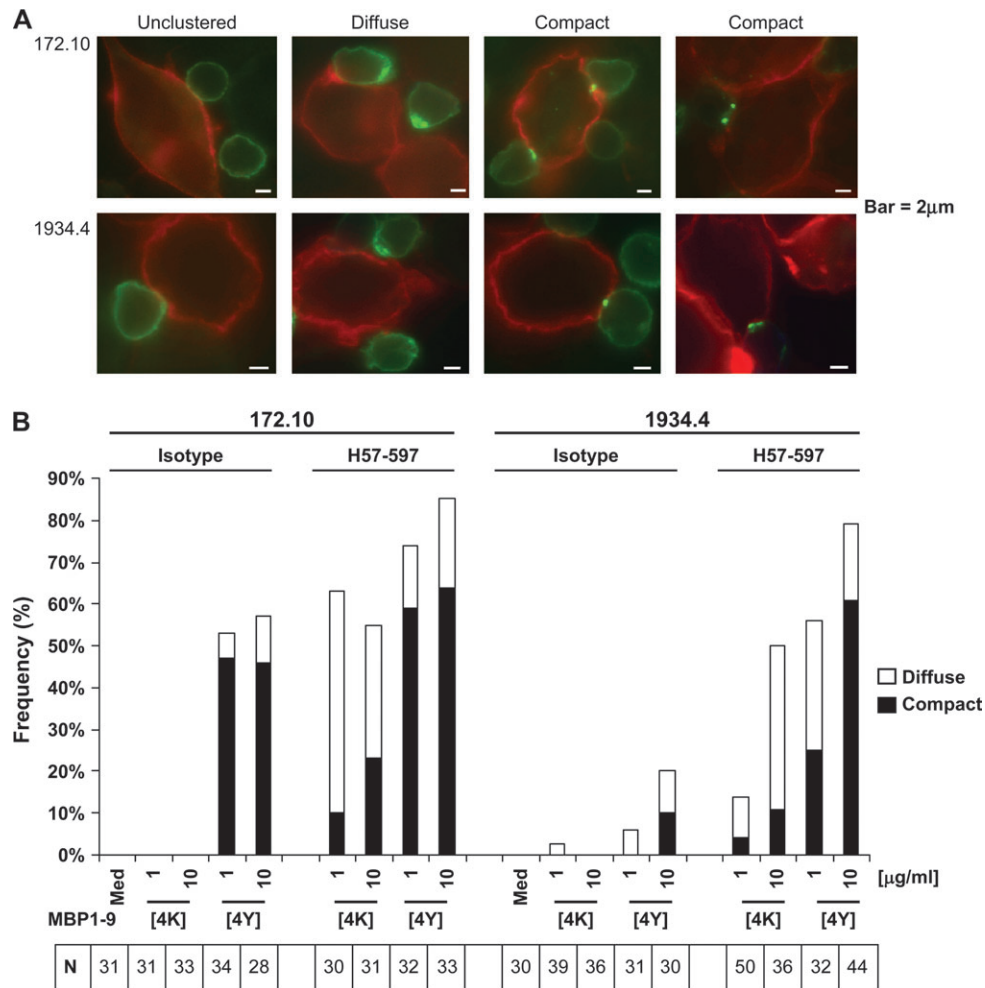
Naive CD4$^+$ 172.10 and 1934.4 tg T cells were purified (in all assays at least 90% were CD62L^{hi}, data not shown) and incubated with peptide-pulsed PL-8 cells [an I-A^u-expressing cell line made by fusing I-A^u splenocytes with the B cell lymphoblastoid line, M12.C3 (37)]. Several different peptide doses were used: 1 or 10 μg ml^{-1} (~0.9 or ~9 μM, respectively) wild-type MBP1–9 or 1 or 10 μg ml^{-1} of the position 4 analog of MBP1–9 in which lysine (K) is substituted by tyrosine (Y). This substitution results in a ~10^3- to 10^4-fold higher affinity for I-A^u without affecting the qualitative nature of T cell recognition, which in turn effectively increases the peptide dose (32–34, 44). The use of both wild-type MBP1–9 and MBP1–9[4Y] resulted in a wide range of effective peptide doses that induced different levels of TCR clustering in an avidity-dependent way (Fig. 2). TCR clustering was categorized as unclustered, diffuse or compact, and representative examples of each class are shown in Fig. 2. In some cases, TCRs clustered into rings rather than circular clusters were seen (Fig. 2) and these were also categorized as compact clusters. Experimental conditions for which no compact clustering was observed following 1 h of stimulation did not

result in significant increases in TCR aggregation after 3 hours of exposure to pMHC (data not shown), suggesting that this is not due to a difference in the rate of clustering. For the higher affinity peptide MBP1–9[4Y], in particular, substantially more TCR clustering was seen for 172.10 tg T cells than for 1934.4 tg T cells (Fig. 2). This difference cannot be accounted for by differences in tg T cell numbers in the CD4$^+$ populations, as ~80% and 70% of CD4$^+$ T cells are antigen specific in 172.10 and 1934.4 TCR tg mice, respectively (Fig. 1).

To enhance the extent of large-scale TCR clustering, we pretreated 1934.4 and 172.10 tg T cells with the anti-Cβ antibody, H57-597, prior to incubation with peptide-pulsed APCs. This antibody is non-mitogenic and in other studies H57-597 Fab fragments have been used to track surface TCRs on CD4$^+$ T cells in the presence of antigen in live cell imaging experiments (4, 10, 45). In addition, in recent live cell imaging studies of auto-antigen-specific T cells in EAE, the use of biotinylated anti-TCR antibodies to analyze TCR clustering did not alter T cell migration (46). To avoid FcγR-mediated cross-linking of TCRs by H57-597, all assays were carried out in the presence of anti-CD16/CD32 antibody and excess isotype-matched hamster antibody of irrelevant specificity (anti-KLH). Thus, based on the recent demonstration that the TCR–CD3 complex is monomeric (47), the effects on TCR clustering that we observe are due to dimerization, rather than multimerization, of the TCRs by H57-597. H57-597 pre-treatment resulted in enhancements in TCR clustering, and these increases were most marked for all peptide doses for 1934.4 tg T cells. For the higher avidity 172.10 tg T cells, greater differences were observed for stimulation with the low-affinity wild-type peptide
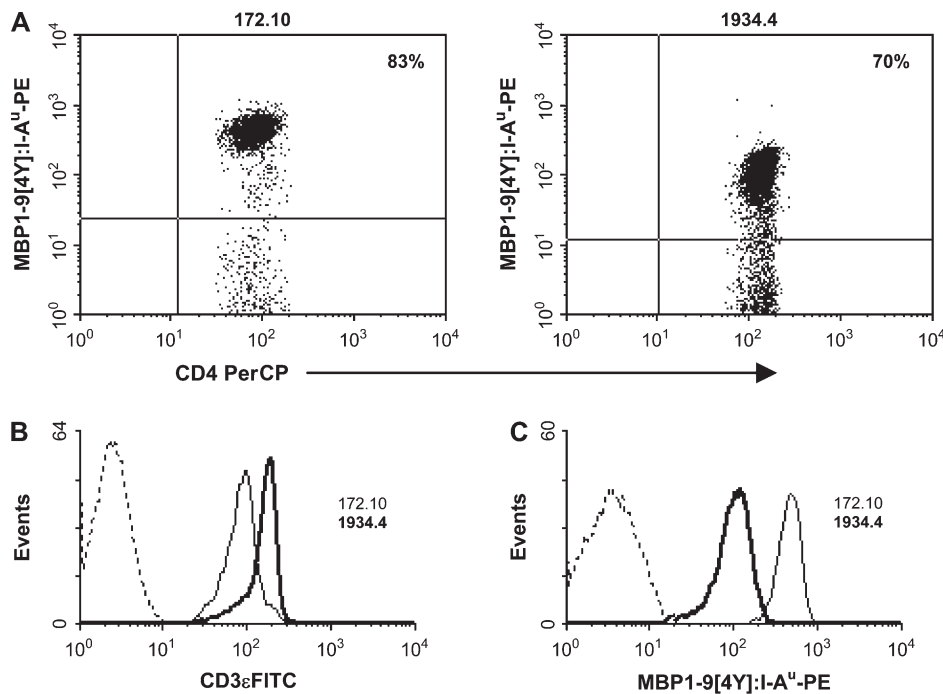
Fig. 1. Binding of fluorescently labeled MBP1–9[4Y]:I-A^u multimers to 172.10 and 1934.4 tg T cells. Splenocytes were incubated with Extravidin–PE-labeled MBP1–9[4Y]:I-A^u multimers and PerCP-labeled anti-CD4 or FITC-labeled anti-CD3ε antibodies as described in Methods. Dot plots of staining of CD4$^+$ cells treated with MBP1–9[4Y]:I-A^u multimers (A) and histogram overlays of TCR levels (B) or multimer staining levels (C) are shown. Dotted lines in (B) and (C) represent the fluorescence levels on the CD3ε-negative (B) and MBP1–9[4Y]:I-A^u multimer-negative (C) populations. The percentages in (A) represent the percentages of CD4$^+$ cells that are typically antigen specific in each of the TCR tg mice.

Fig. 2. TCR clustering on 172.10 and 1934.4 tg T cells. Purified CD4+CD62L^hi cells were treated with either isotype control or Alexa 488-labeled H57-597 and incubated with peptide-pulsed PL-8 cells for 1 h. Cells were washed, fixed and stained with PE-labeled anti-B220 antibody, Cy5-labeled anti-CD4 antibody and, for isotype-treated cells, with Alexa 488-labeled H57-597 as described in Methods. (A) Representative examples of no TCR clustering, diffuse clustering and compact clustering for both 172.10 and 1934.4 tg T cells. Anti-B220 and H57-597 antibody staining are shown in red and green, respectively. All H57-597 positive cells were also CD4+ (data not shown). Bars = 2 μm. (B) Histogram plots of the frequencies at which each type of TCR clustering was observed under different conditions. [4K] = Wild-type MBP1–9 with lysine at position 4 and [4Y] = higher affinity MBP1–9 analog with tyrosine at position 4 (32–34). N = Number of CD4+ T cells analyzed for each condition. Data are representative of at least three independent experiments.

(MBP1–9), that is, under conditions where no or very limited clustering was seen in the absence of H57-597 pre-treatment. The differences in clustering for 172.10 tg T cells using the higher affinity peptide, MBP1–9[4Y], were relatively small, as extensive clustering was observed in the absence of H57-597 pre-treatment (Fig. 2).

Lack of correlation between large-scale TCR clustering and T cell activation

The variations in micrometer-scale TCR clustering shown in Fig. 2 gave us the opportunity to analyze whether there was a correlation between large-scale TCR clustering and T cell activation. For these studies, up-regulation of the early activation markers CD25 and CD69 was assessed. In addition, IL-2 and IFN-γ levels in culture supernatants at 24 and 72 h post-stimulation, respectively, were quantitated.

For 172.10 tg T cells, the marked variations in T cell clustering induced by treatment with 10 μg ml⁻¹ MBP1–9 or 1 μg ml⁻¹ MBP1–9[4Y] (Fig. 2A) do not translate into differences in CD25 or CD69 up-regulation (Fig. 3A–F, open histograms). CD69 was up-regulated more rapidly than CD25 on 172.10 tg T cells, and therefore data for 2 h post-stimulation for CD69 (rather than the 4 h used for CD25) are shown (Fig. 3A and B). The IL-2 and IFN-γ levels observed in response to 10 μg ml⁻¹ MBP1–9 or 1 μg ml⁻¹ MBP1–9[4Y] were also not significantly different (Fig. 3G and H, open histograms, P = 0.34, 0.24, respectively). Further, enhancement of large-scale TCR clustering by H57-597 pre-treatment for cells treated with MBP1–9 resulted in only minor differences in CD25, CD69 up-regulation, and up-regulation approached plateau levels for all antigen doses following 18 and 6 h stimulation, respectively (Fig. 3D and E). H57-597 pre-treatment did not have a significant impact on IL-2 and IFN-γ
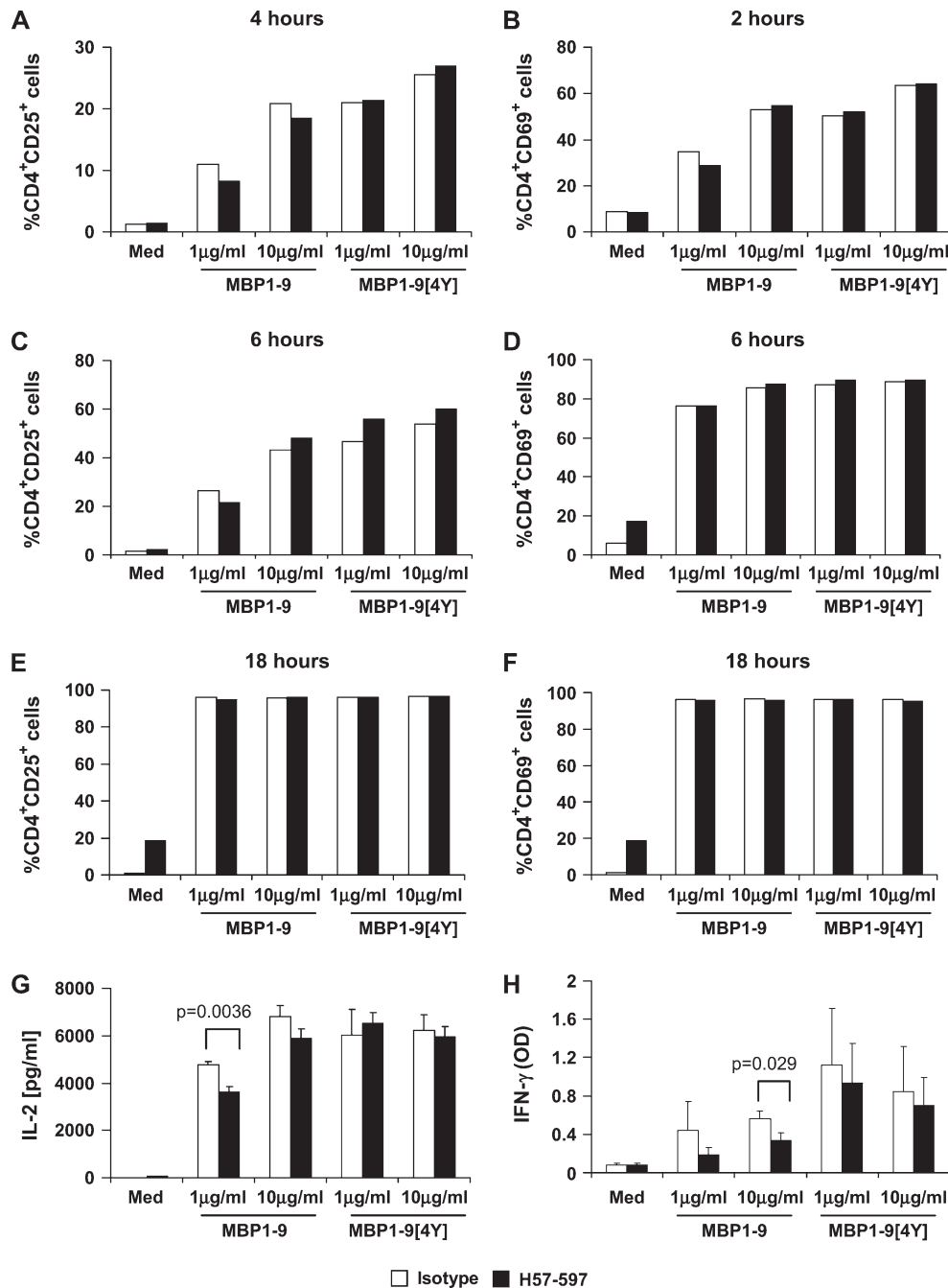
Fig. 3. Up-regulation of CD25 and CD69 (A–F), IL-2 production (G) and IFN-γ production (H) for 172.10 tg T cells following pre-treatment with either isotype control (empty histograms) or H57-597 (filled histograms) and incubation with peptide-pulsed PL-8 cells. (A–F) CD25 and CD69 expression levels following 2, 4, 6 or 18 h incubation (as indicated). Cells were stained with APC-labeled anti-CD25 and FITC-labeled anti-CD69 antibodies. (G) IL-2 levels in culture supernatants following 24 h of stimulation, determined by ELISA. (H) IFN-γ levels in culture supernatants following 72 h of stimulation, determined by ELISA. OD = optical density at 450 nm. For (G) and (H), standard deviations for triplicate samples are indicated by error bars. P values (Student's t-test) for comparisons of cells with isotype control and H57-597 pre-treatment were all >0.05, except for where indicated. Data shown are representative of at least two independent experiments.

production except for small down-modulatory effect (P = 0.0036 for IL-2, P = 0.029 for IFN-γ) in response to 1 μg ml^{-1} (IL-2) or 10 μg ml^{-1} (IFN-γ) MBP1–9 (Fig. 3G and H). Importantly, H57-597 pre-treatment in the absence of peptide resulted in very low levels of CD25/CD69 up-regulation or IL-2 and IFN-γ production (Fig. 3A–H), consistent with the non-

mitogenic nature of this antibody. Taken together, the data for 172.10 tg T cells indicate that the extent of large-scale TCR clustering cannot be used as a predictor of T cell activation.

In contrast to the data for 172.10 tg T cells, incubation of the lower avidity 1934.4 tg T cells with peptide-pulsed APCs results in very limited amounts of large-scale TCR clustering,

even for the higher affinity MBP analog, MBP1–9[4Y] (Fig. 2B). This made it difficult to draw correlations between TCR aggregation and activation. For this reason, we therefore focused our comparative analysis on the activation of these cells under conditions of constant antigen dose, but with and without H57-597 pre-treatment, as the latter treatment greatly increased TCR clustering in response to peptide (Fig. 2B). We

consistently observed that enhancement of TCR clustering by H57-597 pre-treatment resulted in slightly lower levels of CD25 and CD69 up-regulation at 4 and 6 h post-stimulation for all antigen doses (Fig. 4A–D). This was most marked at the lowest antigen dose used (1 μg ml^{-1} MBP1–9). However, differences in CD25 and CD69 up-regulation for H57-597 and isotype control-treated 1934.4 tg cells became negligible
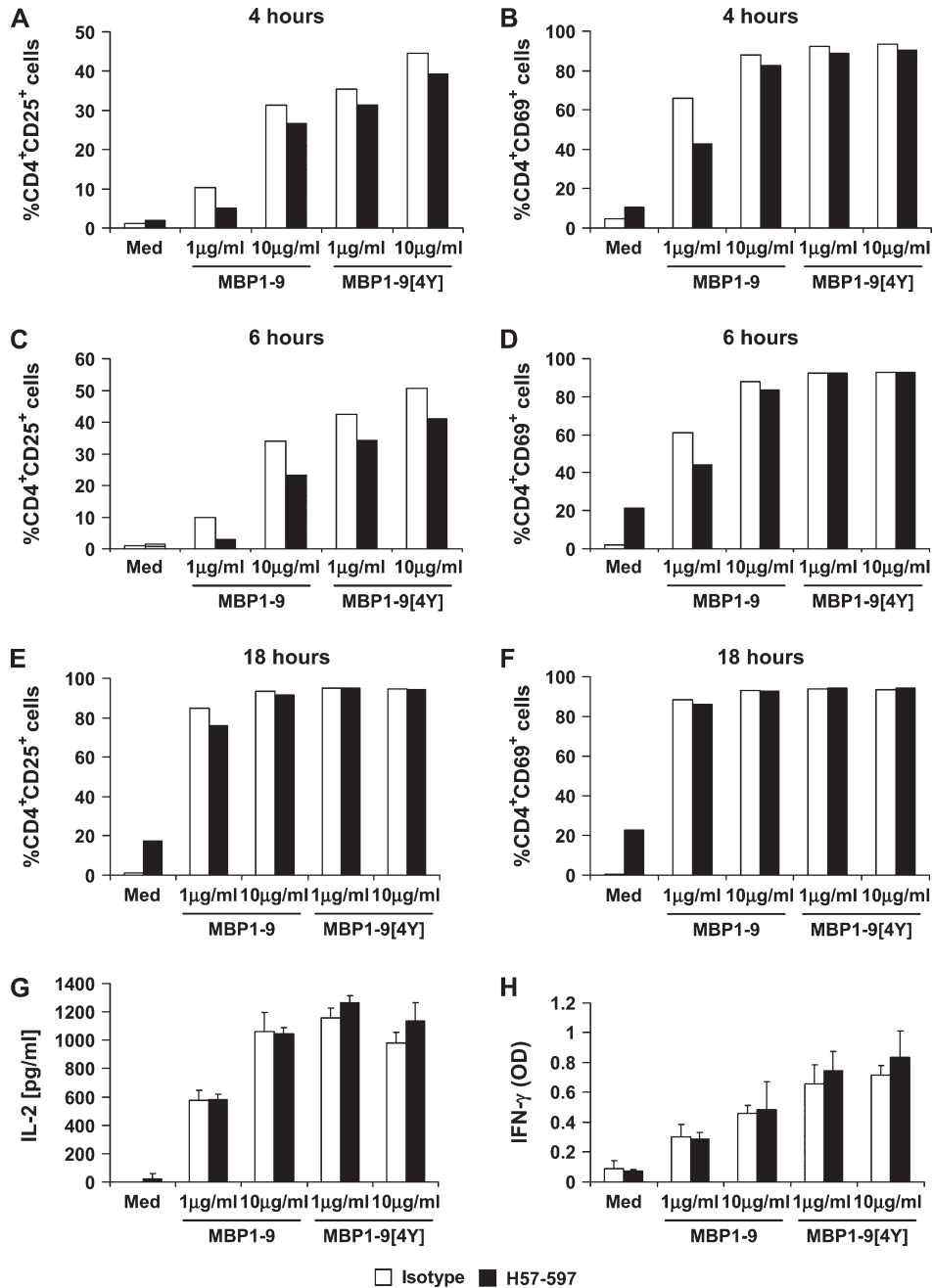
Fig. 4. Up-regulation of CD25 and CD69 (A–F) and IL-2 production (G) and IFN-γ production (H) for 1934.4 tg T cells following pre-treatment with either isotype control (empty histograms) or H57-597 (filled histograms) and incubation with peptide-pulsed PL-8 cells. (A–F) CD25 and CD69 expression levels following 4, 6 or 18 h incubation (as indicated). Cells were stained with APC-labeled anti-CD25 and FITC-labeled anti-CD69 antibodies. (G) IL-2 levels in culture supernatants following 24 h of stimulation, determined by ELISA. (H) IFN-γ levels in culture supernatants following 72 h of stimulation, determined by ELISA. OD = optical density at 450 nm. For (G) and (H), standard deviations for triplicate samples are indicated by error bars. *P* values (Student's *t*-test) for comparisons of cells with isotype control and H57-597 pre-treatment were all >0.05. Data shown are representative of at least two independent experiments.

at 18 h post-stimulation when up-regulation approached maximal levels for all peptide doses (Fig. 4E and F). Analyses of IL-2 or IFN-γ levels in culture supernatants following 24 or 72 h stimulation, respectively, indicated that there were no significant differences between cells treated with H57-597 and isotype control for 1934.4 tg T cells, despite the differences in TCR clustering (Figs 2B, 4G and H). As for 172.10 tg T cells, we observed very low levels of activation of 1934.4 tg T cells that were pre-treated with H57-597 in the absence of stimulatory peptide (Fig. 4).

Analyses of ligand binding and TCR down-regulation for 1934.4 tg T cells

Several possibilities could account for the differences that are observed as a result of H57-597 pre-treatment for CD25 and CD69 up-regulation following stimulation (Figs 3 and 4). First, although unlikely from other studies (4, 45, 48), there might be some partial blockade of TCR–pMHC interactions by H57-597 that might manifest itself, particularly for lower avidity interactions. Second, TCR clustering might result in enhanced TCR internalization that could in turn counteract the positive effect of concentrating TCRs at the TCR–APC interface. As the differences were more marked for 1934.4 tg than for 172.10 tg T cells, we focused our analyses of the potential effects on these tg T cells. To analyze the first possibility, tg T cells were stained with fluorescently labeled pMHC multimers (MBP1–9[4Y]:I-A^u) in the presence or absence of H57-597. In the presence of H57-597, 1934.4 tg T cells stained to slightly higher levels (data not shown) and the multimer dissociated more slowly (Fig. 5A and B). The enhanced binding is most likely due to avidity effects resulting from TCR-induced dimerization by H57-597. The lack of negative effect of H57-597 on pMHC binding is consistent with the structure of an H57-597 Fab fragment complexed with the N15 TCR, where the Fab-binding site is distal to the putative TCR–pMHC interaction site (48).

To investigate the second possibility that H57-597-induced clustering might result in enhanced TCR internalization, 1934.4 tg T cells were stimulated with peptide-pulsed APCs under different conditions (plus/minus H57-597) for 4 h and TCR internalization assessed by staining with anti-CD3ε antibody (145-2C11) (Fig. 5C). Consistent with earlier studies in distinct systems (49–51), there is a direct correlation between effective antigen dose and extent of TCR internalization. For all antigen doses, H57-597 pre-treatment induced slightly greater levels of TCR internalization relative to isotype control-treated cells. These differences in internalization most likely account for the down-modulatory effects of this pre-treatment on CD25 and CD69 up-regulation within several hours of activation. However, this does not appear to impinge upon IL-2, IFN-γ levels or CD25, CD69 up-regulation when assessed at later stages of T cell stimulation (Fig. 4).

Discussion

In the current study, we have analyzed the impact of variations in TCR clustering at the T cell–APC interface on the activation of naive CD4$^+$ T cells. This has been carried out using two MBP1–9:I-A^u-specific T cell populations derived from tg mice
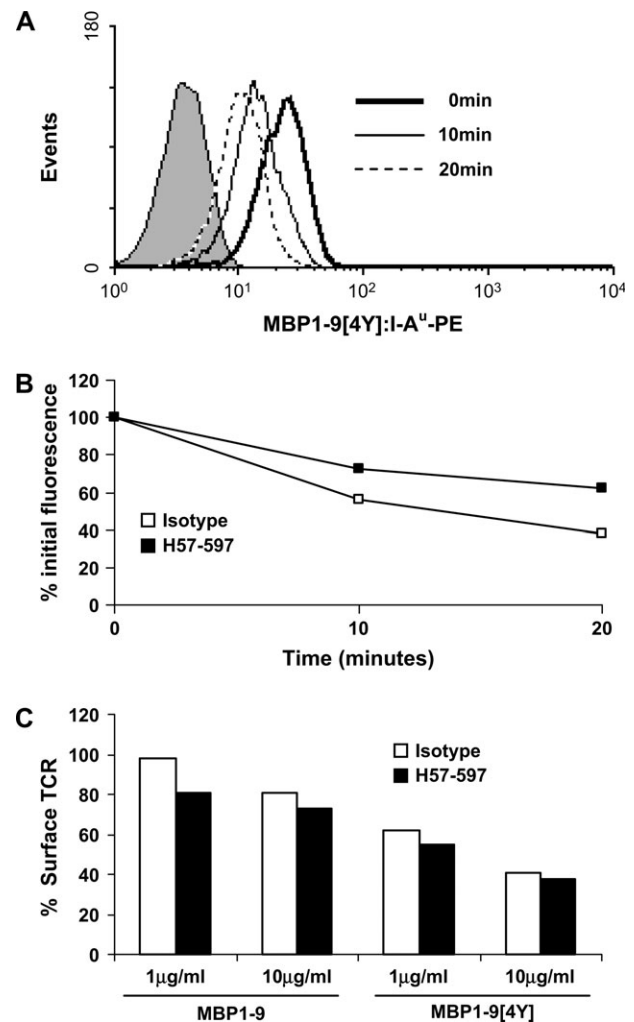
Fig. 5. Binding of MBP1–9[4Y]:I-A^u multimers to 1934.4 tg T cells (A and B) and TCR internalization (C) following pre-treatment with either isotype control (empty histograms) or H57-597 (filled histograms). For (A) and (B), cells were incubated with Extravidin–PE-labeled MBP1–9[4Y]:I-A^u multimers and dissociation in the presence of anti-I-A^u antibody, 10.2.16, assessed. (A) Histogram plots of multimer staining levels for isotype control-treated cells following 0-, 10- and 20-min dissociation, with Extravidin–PE (background) staining indicated by a filled histogram. (B) Plot showing the MFI (background subtracted) at each time point expressed as a percentage of the MFI at 0 min for 1934.4 tg T cells treated with either H57-597 or isotype control. (C) Surface TCR levels on H57-597 or isotype control-treated 1934.4 tg T cells following 4 h stimulation with MBP peptide-pulsed PL-8 cells. The MFI of CD3ε staining on gated CD4$^+$ cells, following treatment, is expressed as the percentage of the MFI for untreated cells (no peptide, isotype control treated) to indicate the % surface TCR. Data in (A–C) are representative of at least two independent experiments.

expressing the 172.10 and 1934.4 TCRs (27, 28). The affinity of the 172.10 TCR for cognate ligand is ~4-fold higher than that of the 1934.4 TCR (36). This system therefore gives us the opportunity to assess the effects of TCR clustering on T cell activation for two well-characterized T cell populations that have the same antigen specificity. The availability of a position 4 analog (MBP1–9[4Y]) that has a 10^3- to 10^4-fold higher affinity for binding to I-A^u (34, 44) has also allowed us to

analyze the effects of varying the effective antigen dose over a wide range.

We show that for higher effective antigen doses (achieved using MBP1–9[4Y]), the 172.10 TCR aggregates more readily at the T cell–APC interface relative to the 1934.4 TCR. This is consistent with the higher affinity of the 172.10 TCR for ligand (36) and with earlier studies demonstrating that the extent of TCR clustering correlates with the avidity of the TCR–pMHC interaction (52). However, the extent of TCR clustering does not correlate well with T cell activation, using CD25 and CD69 up-regulation and IL-2 and IFN-γ production as markers. For example, 0.9 μM MBP1–9[4Y] induces extensive TCR cluster-ing for 172.10 tg T cells, but this does not result in greater responsiveness relative to cells treated with a dose (9 μM) of MBP1–9 that does not induce detectable, large-scale TCR clustering at the T cell–APC interface. Similarly, using distinct antigen recognition systems, a lack of correlation between mature IS formation involving large-scale molecular clustering and the activation of naive and/or *in vitro* primed CD4$^+$ or CD8$^+$ T cells have been reported (14, 22–25), suggesting that our observations are general.

For both doses of the low-affinity, wild-type peptide (MBP1–9) used in the current study, we do not observe large-scale TCR clustering for 1934.4 and 172.10 tg T cells. Despite this, activation is relatively efficient, indicating that TCR clustering on a large scale is not a prerequisite for the activation of naive CD4$^+$ cells. However, we cannot exclude the induction of 'micro' clusters of TCRs comprising very small numbers of receptors that would be difficult to characterize due to the relatively high level of cell surface TCR expression. It is also possible that under stimulation conditions that do not induce large-scale TCR clustering, re-organization of other compo-nents, such as LFA-1/ICAM-1 or talin, at the T cell–APC in-terface occurs. This would be consistent with observations that an ICAM-1 ring is observed when TCRs are clustered at the T cell–APC interface in response to only 10 agonist pMHC complexes (20), and that talin/LFA-1 re-organization has a lower stimulatory threshold relative to large-scale TCR clustering (26).

Taken together with earlier studies (16–22), our analyses indicate that TCR scanning of ligands is a highly efficient process. In general, the levels of cognate (agonist) pMHC ligand to which T cells are exposed under physiological conditions might be expected to be too low to induce large-scale TCR clustering, and our studies, therefore, have relevance to understanding T cell activation *in vivo*. In this context, substantial TCR signaling can occur when naive T cells serially contact different APCs in lymph nodes (53–55). It has not yet been possible to determine whether large-scale TCR aggregation and/or IS formation occurs during T cell–dendritic cell interactions in lymph nodes observed using intravital microscopy (56). It is therefore conceivable that although naive T cells can form stable conjugates with APCs such as dendritic cells following a period of making serial, short-lived contacts (55), extensive TCR clustering at the T cell–APC interface does not occur *in vivo*. However, this does not exclude the possibility that other features, such as cytoskeletal rearrangements, of the IS are present in these T cell–APC conjugates.

The limited extent of micrometer-scale TCR clustering for both doses of the low- and high-affinity peptides (MBP1–9

and MBP1–9[4Y], respectively) in the 1934.4 TCR system and for the low-affinity peptide, MBP1–9, in the 172.10 TCR sys-tem prompted us to enhance TCR clustering by incuba-ting cells with the non-mitogenic anti-Cβ antibody, H57-597 (39). The purpose of this was to investigate a possible effect of alterations in TCR clustering on T cell activation, particularly for 1934.4 tg T cells where very limited TCR aggregation was observed at all peptide doses without H57-597 pre-treatment. The H57-597 antibody was chosen, since based on a recent model for the organization of the TCR–CD3 complex demonstrating that the complex is monomeric (47), it would be predicted to dimerize, rather than multimerize, TCRs. We show that H57-597 does not negatively affect pMHC binding, consistent with earlier structural studies of the N15 TCR in which H57-597 was shown to bind distally to the putative antigen-binding site (48). In addition, Fab fragments of H57-597 have been used by others to track TCRs on CD4$^+$ cells in live cell imaging experiments (4, 10, 45). The use of this antibody therefore gave us the possibility to assess activation of T cells under conditions where the amount of TCR clustering at the T cell–APC interface was altered in the presence of constant antigen doses. Further, recent studies using biotinylated anti-TCR antibodies to track TCRs on autoreactive, live T cells in an EAE model indicated that this treatment does not affect T cell motility (46), providing support that our approach does not have undesirable effects on T cell properties. Depending on the timing and marker of activation used, we observe mixed effects of variations in the extent of TCR clustering on T cell activation. In all cases, however, when effects are observed, they are modest. For example, for early T cell activation events such as CD25 and CD69 up-regulation (following 2–4 h stimulation), the up-regulation of these proteins following exposure to the same antigen dose shows some dependence on the extent of TCR clustering. The effects are most marked for the lower avidity 1934.4 tg T cells. However, rather than a direct correlation, if an effect of TCR clustering is observed, the extent of ag-gregation inversely correlates with CD25/CD69 up-regulation. Although this might appear to be counterintuitive, it is in accordance with the report that TCR aggregation in the IS serves to down-regulate TCR signaling by enhancing TCR internalization (15). Consistent with this, we also observe slight increases in TCR internalization for 1934.4 tg T cells that are pre-treated with H57-597. However, and perhaps most importantly from the point of view of T cell effector function, even when differences are observed for 1934.4 tg T cells for early activation marker expression at 4 h post-stimulation, these do not translate into variations in IL-2 or IFN-γ levels at 24 and 72 h, respectively, or in CD69 or CD25 up-regulation at 18 h.

In summary, using naive T cells bearing two MBP1–9:I-A^u-specific TCRs of distinct affinities, we have shown that the extent of TCR clustering at the T cell–APC interface cannot be used to predict the level of T cell activation when markers such as CD25 and CD69 up-regulation and cytokine production are used. In addition, extensive TCR clustering is not required for efficient T cell stimulation, consistent with studies, indicating that very few pMHC complexes are needed to trigger a T cell (16–22). Our data therefore provide insight into the parameters that lead to naive T cell activation in murine EAE.

Acknowledgements

Abbreviations

APC	antigen-presenting cell
cSMAC	central supramolecular activation cluster
EAE	experimental autoimmune encephalomyelitis
IS	immunological synapse
KLH	keyhole limpet hemocyanin
LFA	leukocyte function-associated antigen
MFI	mean fluorescence intensity
PKC	protein kinase C
pMHC	peptide–MHC
tg	transgenic

References

1 Monks, C. R., Freiberg, B. A., Kupfer, H., Sciaky, N. and Kupfer, A. 1998. Three-dimensional segregation of supramolecular activation clusters in T cells. *Nature* 395:82.

2 Grakoui, A., Bromley, S. K., Sumen, C. *et al.* 1999. The immunological synapse: a molecular machine controlling T cell activation. *Science* 285:221.

3 Wülfing, C., Sjaastad, M. D. and Davis, M. M. 1998. Visualizing the dynamics of T cell activation: intracellular adhesion molecule 1 migrates rapidly to the T cell/B cell interface and acts to sustain calcium levels. *Proc. Natl Acad. Sci. USA* 95:6302.

4 Dustin, M. L. and Cooper, J. A. 2000. The immunological synapse and the actin cytoskeleton: molecular hardware for T cell signaling. *Nat. Immunol.* 1:23.

5 Freiberg, B. A., Kupfer, H., Maslanik, W. *et al.* 2002. Staging and resetting T cell activation in SMACs. *Nat. Immunol.* 3:911.

6 Davis, D. M. 2002. Assembly of the immunological synapse for T cells and NK cells. *Trends Immunol.* 23:356.

7 Wang, H., McCann, F. E., Gordan, J. D. *et al.* 2004. ADAP-SLP-76 binding differentially regulates supramolecular activation cluster (SMAC) formation relative to T cell-APC conjugation. *J. Exp. Med.* 200:1063.

8 Choudhuri, K., Wiseman, D., Brown, M. H., Gould, K. and van der Merwe, P. A. 2005. T-cell receptor triggering is critically dependent on the dimensions of its peptide-MHC ligand. *Nature* 436:578.

9 Yokosuka, T., Sakata-Sogawa, K., Kobayashi, W. *et al.* 2005. Newly generated T cell receptor microclusters initiate and sustain T cell activation by recruitment of Zap70 and SLP-76. *Nat. Immunol.* 6:1253.

10 Campi, G., Varma, R. and Dustin, M. L. 2005. Actin and agonist MHC-peptide complex-dependent T cell receptor microclusters as scaffolds for signaling. *J. Exp. Med.* 202:1031.

11 Bromley, S. K., Iaboni, A., Davis, S. J. *et al.* 2001. The immunological synapse and CD28-CD80 interactions. *Nat. Immunol.* 2:1159.

12 Holdorf, A. D., Lee, K. H., Burack, W. R., Allen, P. M. and Shaw, A. S. 2002. Regulation of Lck activity by CD4 and CD28 in the immunological synapse. *Nat. Immunol.* 3:259.

13 Boisvert, J., Edmondson, S. and Krümmel, M. F. 2004. Immunological synapse formation licenses CD40-CD40L accumulations at T-APC contact sites. *J. Immunol.* 173:3647.

14 Purtic, B., Pitcher, L. A., van Oers, N. S. and Wülfing, C. 2005. T cell receptor (TCR) clustering in the immunological synapse integrates TCR and costimulatory signaling in selected T cells. *Proc. Natl Acad. Sci. USA* 102:2904.

15 Lee, K. H., Dinner, A. R., Tu, C. *et al.* 2003. The immunological synapse balances T cell receptor signaling and degradation. *Science* 302:1218.

16 Demotz, S., Grey, H. M. and Sette, A. 1990. The minimal number of class II MHC-antigen complexes needed for T cell activation. *Science* 249:1028.

17 Harding, C. V. and Unanue, E. R. 1990. Quantitation of antigen-presenting cell MHC class II/peptide complexes necessary for T-cell stimulation. *Nature* 346:574.

18 Kimachi, K., Croft, M. and Grey, H. M. 1997. The minimal number of antigen-major histocompatibility complex class II complexes required for activation of naive and primed T cells. *Eur. J. Immunol.* 27:3310.

19 Reay, P. A., Matsui, K., Haase, K., Wülfing, C., Chien, Y. H. and Davis, M. M. 2000. Determination of the relationship between T cell responsiveness and the number of MHC-peptide complexes using specific monoclonal antibodies. *J. Immunol.* 164:5626.

20 Irvine, D. J., Purbhoo, M. A., Krogsgaard, M. and Davis, M. M. 2002. Direct observation of ligand recognition by T cells. *Nature* 419:845.

21 Krogsgaard, M., Li, Q. J., Sumen, C., Huppa, J. B., Huse, M. and Davis, M. M. 2005. Agonist/endogenous peptide-MHC hetero-dimers drive T cell activation and sensitivity. *Nature* 434:238.

22 Purbhoo, M. A., Irvine, D. J., Huppa, J. B. and Davis, M. M. 2004. T cell killing does not require the formation of a stable mature immunological synapse. *Nat. Immunol.* 5:524.

23 O'Keefe, J. P., Blaine, K., Alegre, M. L. and Gajewski, T. F. 2004. Formation of a central supramolecular activation cluster is not required for activation of naive CD8+ T cells. *Proc. Natl Acad. Sci. USA* 101:9351.

24 O'Keefe, J. P. and Gajewski, T. F. 2005. Cutting edge: cytotoxic granule polarization and cytolysis can occur without central supramolecular activation cluster formation in CD8+ effector T cells. *J. Immunol.* 175:5581.

25 Faroudi, M., Utzny, C., Salio, M. *et al.* 2003. Lytic versus stimulatory synapse in cytotoxic T lymphocyte/target cell interaction: manifestation of a dual activation threshold. *Proc. Natl Acad. Sci. USA* 100:14145.

26 Kupfer, A. and Singer, S. J. 1989. The specific interaction of helper T cells and antigen-presenting B cells. IV. Membrane and cytoskeletal reorganizations in the bound T cell as a function of antigen dose. *J. Exp. Med.* 170:1697.

27 Goverman, J., Woods, A., Larson, L., Weiner, L. P., Hood, L. and Zaller, D. M. 1993. Transgenic mice that express a myelin basic protein-specific T cell receptor develop spontaneous autoimmunity. *Cell* 72:551.

28 Pearson, C. I., van Ewijk, W. and McDevitt, H. O. 1997. Induction of apoptosis and T helper 2 (Th2) responses correlates with peptide affinity for the major histocompatibility complex in self-reactive T cell receptor transgenic mice. *J. Exp. Med.* 185:583.

29 Zamvil, S. S., Mitchell, D. J., Moore, A. C., Kitamura, K., Steinman, L. and Rothbard, J. B. 1986. T-cell epitope of the autoantigen myelin basic protein that induces encephalomyelitis. *Nature* 324:258.

30 Acha-Orbea, H., Mitchell, D. J., Timmermann, L. *et al.* 1988. Limited heterogeneity of T cell receptors from lymphocytes mediating autoimmune encephalomyelitis allows specific immune intervention. *Cell* 54:263.

31 Urban, J. L., Kumar, V., Kono, D. H. *et al.* 1988. Restricted use of T cell receptor V genes in murine autoimmune encephalomyelitis raises possibilities for antibody therapy. *Cell* 54:577.

32 Fairchild, P. J., Wildgoose, R., Atherton, E., Webb, S. and Wraith, D. C. 1993. An autoantigenic T cell epitope forms unstable complexes with class II MHC: a novel route for escape from tolerance induction. *Int. Immunol.* 5:1151.

33 Mason, K., Denney, D. W. J. and McConnell, H. M. 1995. Myelin basic protein peptide complexes with the class II MHC molecules I-A^u and I-A^k form and dissociate rapidly at neutral pH. *J. Immunol.* 154:5216.

34 Fugger, L., Liang, J., Gautam, A., Rothbard, J. B. and McDevitt, H. O. 1996. Quantitative analysis of peptides from myelin basic protein binding to the MHC class II protein, I-A^u, which confers susceptibility to experimental allergic encephalomyelitis. *Mol. Med.* 2:181.

35 Liu, G. Y., Fairchild, P. J., Smith, R. M., Prowle, J. R., Kioussis, D. and Wraith, D. C. 1995. Low avidity recognition of self-antigen by T cells permits escape from central tolerance. *Immunity* 3:407.

36 Garcia, K. C., Radu, C., Ho, J., Ober, R. J. and Ward, E. S. 2001. Kinetics and thermodynamics of T cell receptor-autoantigen interactions in murine experimental autoimmune encephalomyelitis. *Proc. Natl Acad. Sci. USA* 98:6818.

37 Wraith, D. C., Smilek, D. E. and Webb, S. 1992. MHC-binding peptides for immunotherapy of experimental autoimmune disease. *J. Autoimmun.* 5(Suppl. A):103.

38 Wraith, D. C., Smilek, D. E., Mitchell, D. J., Steinman, L. and McDevitt, H. O. 1989. Antigen recognition in autoimmune encephalomyelitis and the potential for peptide-mediated immunotherapy. *Cell* 59:247.

39 Kubo, R. T., Born, W., Kappler, J. W., Marrack, P. and Pigeon, M. 1989. Characterization of a monoclonal antibody which detects all murine alpha beta T cell receptors. *J. Immunol.* 142:2736.

40 Oi, V. T., Jones, P. P., Goding, J. W. and Herzenberg, L. A. 1978. Properties of monoclonal antibodies to mouse Ig allotypes, H-2, and Ia antigens. *Curr. Top. Microbiol. Immunol.* 81:115.

41 Radu, C. G., Ober, B. T., Colantonio, L., Qadri, A. and Ward, E. S. 1998. Expression and characterization of recombinant soluble peptide:I-A complexes associated with murine experimental autoimmune diseases. *J. Immunol.* 160:5915.

42 Radu, C. G., Anderton, S. M., Firan, M., Wraith, D. C. and Ward, E. S. 2000. Detection of autoreactive T cells in H-2^u mice using peptide-MHC multimers. *Int. Immunol.* 12:1553.

43 Ober, R. J., Martinez, C., Vaccaro, C., Zhou, J. and Ward, E. S. 2004. Visualizing the site and dynamics of IgG salvage by the MHC class I-related receptor, FcRn. *J. Immunol.* 172:2021.

44 Anderton, S. M., Radu, C. G., Lowrey, P. A., Ward, E. S. and Wraith, D. C. 2001. Negative selection during the peripheral immune response to antigen. *J. Exp. Med.* 193:1.

45 Moss, W. C., Irvine, D. J., Davis, M. M. and Krümmel, M. F. 2002. Quantifying signaling-induced reorientation of T cell receptors during immunological synapse formation. *Proc. Natl Acad. Sci. USA* 99:15024.

46 Kawakami, N., Nagerl, U. V., Odoardi, F., Bonhoeffer, T., Wekerle, H. and Flügel, A. 2005. Live imaging of effector cell trafficking and autoantigen recognition within the unfolding autoimmune encephalomyelitis lesion. *J. Exp. Med.* 201:1805.

47 Call, M. E., Pyrdol, J., Wiedmann, M. and Wucherpfennig, K. W. 2002. The organizing principle in the formation of the T cell receptor-CD3 complex. *Cell* 111:967.

48 Wang, J., Lim, K., Smolyar, A. *et al.* 1998. Atomic structure of an alphabeta T cell receptor (TCR) heterodimer in complex with an anti-TCR Fab fragment derived from a mitogenic antibody. *EMBO J.* 17:10.

49 Valitutti, S., Muller, S., Cella, M., Padovan, E. and Lanzavecchia, A. 1995. Serial triggering of many T-cell receptors by a few peptide-MHC complexes. *Nature* 375:148.

50 Bachmann, M. F., Oxenius, A., Speiser, D. E. *et al.* 1997. Peptide-induced T cell receptor down-regulation on naive T cells predicts agonist/partial agonist properties and strictly correlates with T cell activation. *Eur. J. Immunol.* 27:2195.

51 Itoh, Y., Hemmer, B., Martin, R. and Germain, R. N. 1999. Serial TCR engagement and down-modulation by peptide:MHC molecule ligands: relationship to the quality of individual TCR signaling events. *J. Immunol.* 162:2073.

52 Grakoui, A., Bromley, S. K., Sumen, C. *et al.* 1999. The immunological synapse: a molecular machine controlling T cell activation. *Science* 285:221.

53 Miller, M. J., Wei, S. H., Parker, I. and Cahalan, M. D. 2002. Two-photon imaging of lymphocyte motility and antigen response in intact lymph node. *Science* 296:1869.

54 Miller, M. J., Safrina, O., Parker, I. and Cahalan, M. D. 2004. Imaging the single cell dynamics of CD4$^+$ T cell activation by dendritic cells in lymph nodes. *J. Exp. Med.* 200:847.

55 Mempel, T. R., Henrickson, S. E. and Von Andrian, U. H. 2004. T-cell priming by dendritic cells in lymph nodes occurs in three distinct phases. *Nature* 427:154.

56 Sumen, C., Mempel, T. R., Mazo, I. B. and Von Andrian, U. H. 2004. Intravital microscopy: visualizing immunity in context. *Immunity* 21:315.